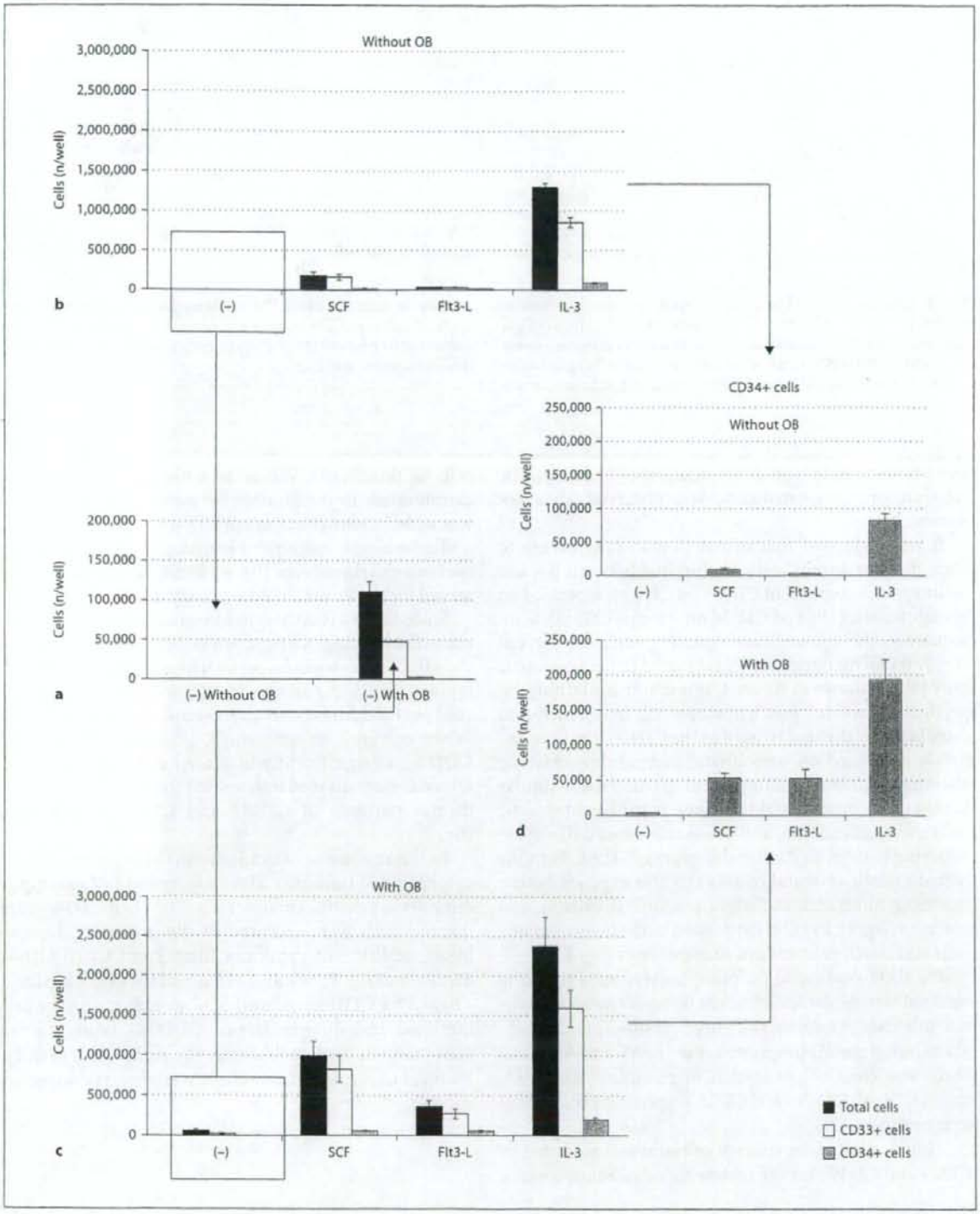
Without OB
Cells (n/well)
3,000,000
2,500,000
2,000,000
1,500,000
1,000,000
500,000
0
b
(–)
SCF
Flt3-L
IL-3
CD34+ cells
Without OB
250,000
200,000
150,000
100,000
50,000
0
(–)
SCF
Flt3-L
IL-3
200,000
150,000
100,000
50,000
0
a
(–) Without OB
(–) With OB
With OB
d
With OB
c
Total cells
CD33+ cells
CD34+ cells

3

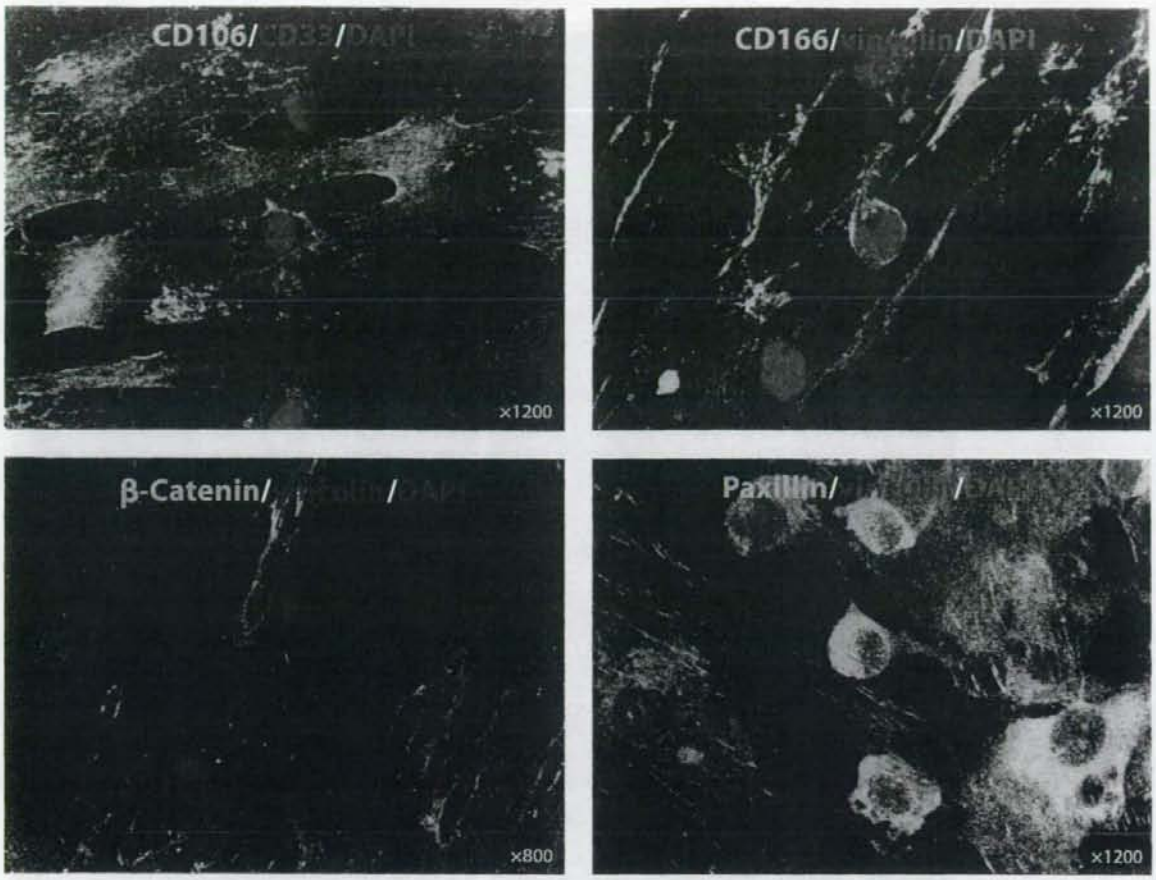

Fig. 4. Immunohistochemical analysis of the interaction between osteoblasts and human CD34+ bone marrow cells. Human CD34+ bone marrow cells were grown on a primary culture of osteoblasts for 2 weeks and examined as in figure 1b.

Fig. 3. Effect of human osteoblasts and cytokines on the growth and differentiation of human CD34+ bone marrow cells. Human CD34+ bone marrow cells were cultured with or without human osteoblasts (OB) for 2 weeks in the presence or absence of the cytokines indicated. After cultivation, the ensuing hematopoietic cells were collected, counted, and positivity for CD33 and CD34 was determined by flow cytometry. The actual total cell numbers and the numbers of cells in each subpopulation are represented by bar graphs. **a** With or without OB (in the absence of cytokines); **b** without OB (in the presence of cytokines); **c** with OB (in the presence of cytokines); **d** CD34+ cells extracted from **b** and **c**.

Discussion

As reported in this paper, when cultured on human osteoblasts, human CD34+ bone marrow cells were able to survive without the addition of any cytokine, and differentiated into myeloid cells with slight proliferation, suggesting that human osteoblasts possess the ability to support the survival and differentiation of hematopoietic cells in vitro. Analysis by confocal microscopy suggested that cell adhesion molecules, including CD29/49d, CD106, and CD166, are involved in cell-to-cell interaction between hematopoietic cells and osteoblasts. Since we observed that FAK and AKT were colocalized with CD29/

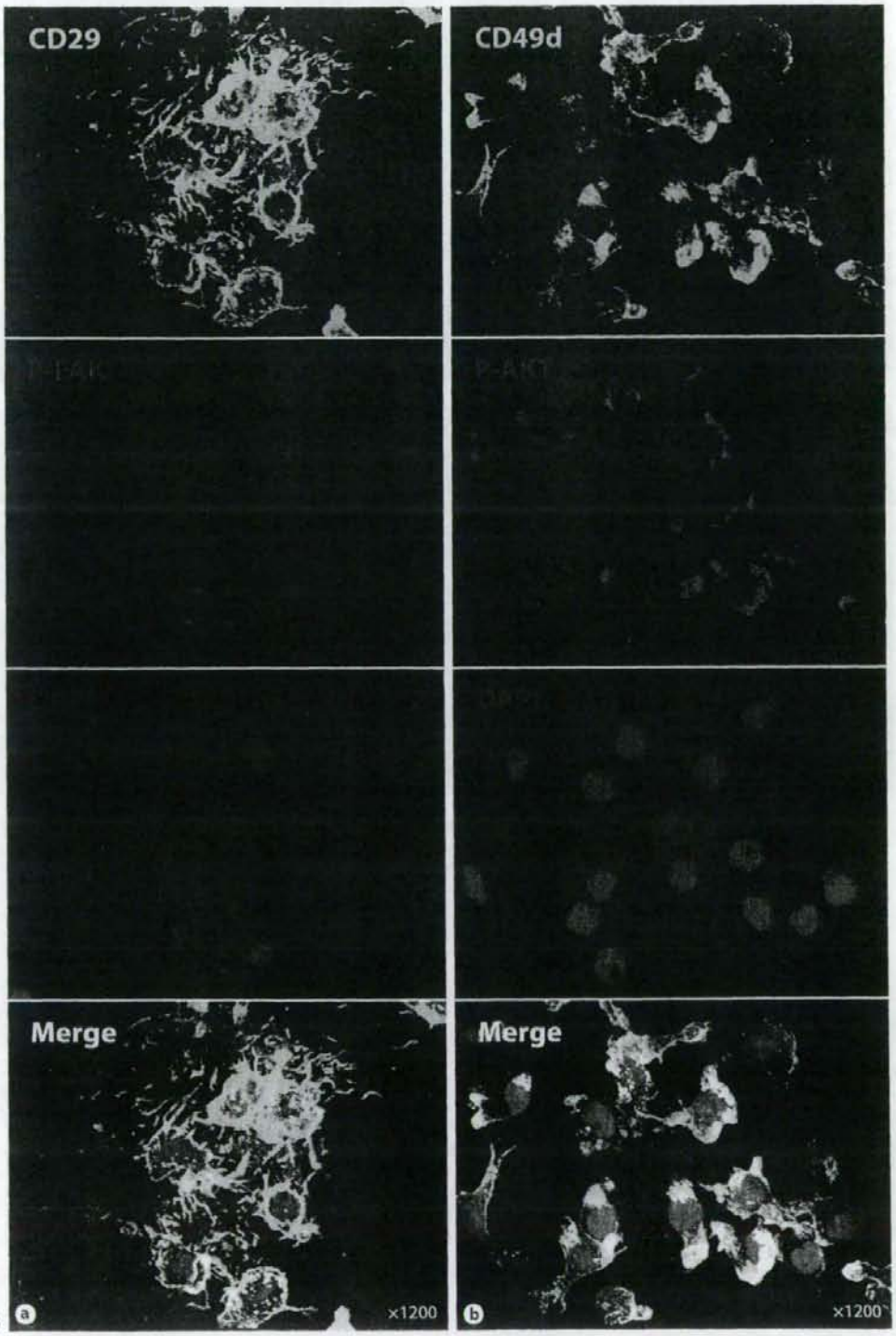

5

49d and phosphorylated in hematopoietic cells adhering to osteoblasts, we suspect that cell-to-cell interaction induces activation of integrin-bound kinases, leading to cell survival signals in hematopoietic cells in which AKT is involved. Although CD34+ bone marrow cells were cultured in the presence of 30% of the cultured supernatant of osteoblasts, most cells died over a 4-week culture period (data not shown), suggesting that the soluble factors derived from osteoblasts are not sufficient to support the survival of human CD34+ bone marrow cells, and adhesion to osteoblasts must be important for the survival of hematopoietic cells.

Human osteoblasts have been reported to produce several hematopoietic cytokines, including IL-1β, IL-6, IL-7, G-CSF, M-CSF, GM-CSF, tumor necrosis factor-α, LIF, OPG, receptor activator of NF-κB ligand, SDF-1, VEGF, and osteoclast differentiation factor [1, 2, 10–12], and not to produce IL-1α, IL-3, or SCF [10]. However, in our experiment, human osteoblasts did not produce IL-7, G-CSF, M-CSF, or GM-CSF. Although the precise reason for the discrepancy is not clear, it may be attributable to differences in cell culture conditions or donor age. Alternatively, different subsets or differentiation states related to differential cytokine production may be present among the osteoblasts.

Several cytokines have been shown to contribute to the maintenance, proliferation, and differentiation of HSCs. For example, Flt3-L and SCF play an important role in the early stage of hematopoiesis [13]. An in vivo study has demonstrated that SCF and IL-3 prevent unirradiated hematopoietic progenitors from undergoing apoptosis, and Flt3-L has been demonstrated to induce survival and proliferation of CD34+CD38– cells [14], suggesting the effects of these cytokines on hematopoiesis in vivo to some extent [15], but their effects in vitro, whether alone or in combination, are still a matter of controversy [2]. The results of this study demonstrate that SCF and IL-3, but not Flt3-L, induce proliferation of CD34+ bone marrow cells to some extent in our culture condition. When added to the coculture system of human osteoblasts and human CD34+ bone marrow cells, however, each of them significantly promoted the proliferation of hematopoietic cells. SCF and Flt3-L induced in particular significant growth of hematopoietic cells cultured on osteoblasts. Since our RT-PCR experiments revealed no expression of SCF and IL-3 mRNA in osteoblasts, the major role of osteoblasts in hematopoiesis could be to maintain HSCs as HSCs and therefore the lack of proliferation-inducing cytokines is appropriate for this role. In the context of the microenvironment, other cells should supply these factors to the niche. Alternatively, it is also possible that disaggregated osteoblasts do not produce these factors when they are grown in monocultures but do so in the niche when in the appropriate context.

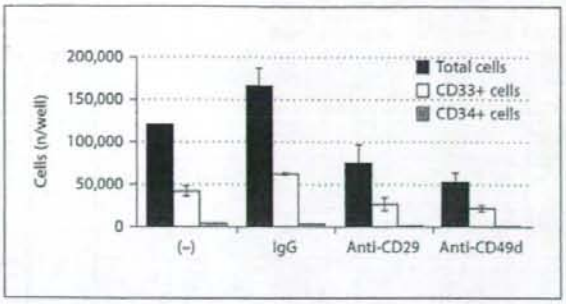

Fig. 6. Effect of anti-integrin antibodies on growth of CD34+ bone marrow cells on human osteoblasts. Human CD34+ bone marrow cells were cultured on osteoblasts for 2 weeks in the presence or absence of antibodies against CD29 or CD49d at a concentration of 5 μg/ml. Following cultivation, hematopoietic cells were collected, counted, and positivity for CD33 and CD34 was determined by flow cytometry (see fig. 3). Purified mouse IgG served as a negative control.

CD184, a receptor for CXC subfamily chemokines, was originally identified as an orphan receptor [16]. It was suggested that CD184 and its sole ligand SDF-1 play an important role in hematopoiesis and are required for homing of stem cells and progenitor cells from the liver to the bone marrow [2, 16–18], but their role at the molecular level remains unknown. Tokoyoda et al. [18] stated that contact between the earliest HSCs and SDF-1-expressing cells is necessary for B lymphopoiesis. In our study, the CD184 expression pattern was dramatically altered by cytokines and the presence of osteoblasts. Although the exact mechanism of action remains to be elucidated, the different expression pattern of CD184 may be related to the different function of hematopoietic cells,

Fig. 5. Phosphorylation of cell signaling molecules in hematopoietic cells cultured on osteoblasts detected by immunohistochemistry. Human CD34+ bone marrow cells were grown on a primary culture of osteoblasts for 2 weeks and stained with the combination of phospho-specific antibodies and anti-cell adhesion molecule antibodies and examined as in figure 4. **a** CD29 versus phosphorylated FAK; **b** CD49d versus phosphorylated AKT.

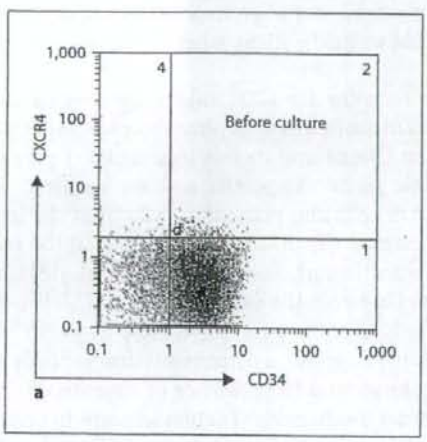

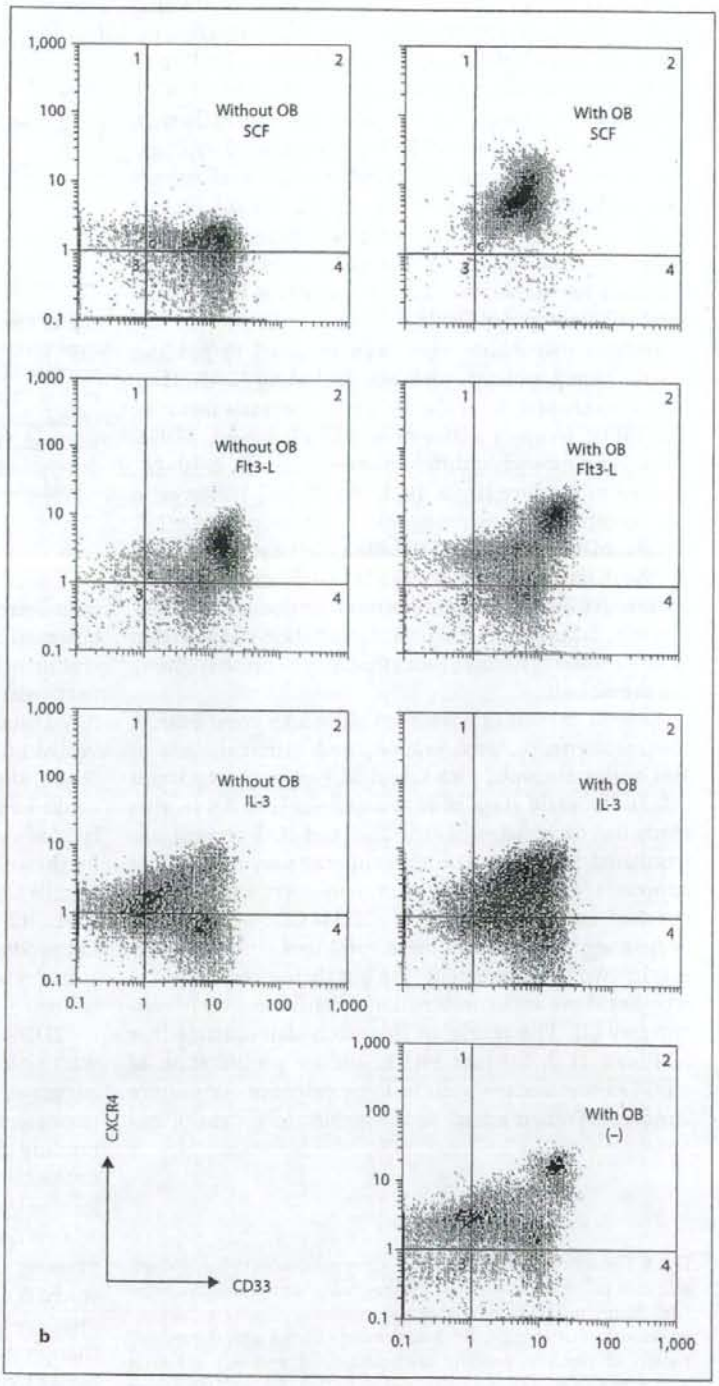

Fig. 7. Expression of CD184 in hematopoietic cells grown on human osteoblasts. Human CD34+ bone marrow cells were cultured for 2 weeks (see fig. 3). Hematopoietic cells were collected and examined by flow cytometry. Two-parameter histograms for CD184 versus CD34 (**a**) or CD33 (**b**) are shown.

e.g. homing. Further investigation to identify the role of CD184 expression in hematopoiesis is now underway.

In conclusion, human osteoblasts have the ability to support the survival and differentiation of human CD34+ bone marrow cells. Addition of cytokines to this culture system stimulates human CD34+ bone marrow cells to differentiate into various blood cells. Osteoblasts provide a useful in vitro model of the hematopoietic microenvironment, and further studies are required to elucidate the role of the microenvironment in early hematopoiesis.

Acknowledgments

This work was supported in part by the 3rd-Term Comprehensive 10-Year-Strategy for Cancer Control, Research on Children and Families, Research on Human Genome Tailor Made and Research on Publicly Essential Drugs and Medical Devices, Health and Labor Sciences Research Grants from the Ministry of Health, Labor and Welfare of Japan and a grant from the Japanese Health Sciences Foundation for Research on Health Sciences Focusing on Drug Innovation. A part of this study was also financially supported by the Budget for Nuclear Research of the Ministry of Education, Culture, Sports, Science and Technology, based on the screening and counseling by the Atomic Energy.

References

1 Taichman RS, Emerson SG: The role of osteoblasts in the hematopoietic microenvironment. Stem Cells 1998;16:7–15.

2 Taichman RS: Blood and bone: two tissues whose fates are intertwined to create the hematopoietic stem-cell niche. Blood 2005;105:2631–2649.

3 Zhang J, Niu C, Ye L, Ye L, Huang H, He X, Tong WG, Ross J, Haug J, Johnson T, Feng JQ, Harris S, Wiedemann LM, Mishina Y, Li L: Identification of the haematopoietic stem cell niche and control of the niche size. Nature 2003;425:836–841.

4 Calvi LM, Adams GB, Weibrecht KW, Weber JM, Olson DP, Knight MC, Martin RP, Schipani E, Divieti P, Bringhurst FR, Milner LA, Kronenberg HM, Scadden DT: Osteoblastic cells regulate the haematopoietic stem cell niche. Nature 2003;425:841–846.

5 Arai F, Hirao A, Ohmura M, Sato H, Matsuoka S, Takubo K, Ito K, Koh GY, Suda T: Tie2/angiopoietin-1 signaling regulates hematopoietic stem cell quiescence in the bone marrow niche. Cell 2004;118:149–161.

6 Saito M, Kiyokawa N, Taguchi T, Suzuki K, Sekino T, Mimori K, Suzuki T, Nakajima H, Katagiri YU, Fujimura J, Fujita H, Ishimoto K, Yamashiro Y, Fujimoto J: Granulocyte colony-stimulating factor directly affects human monocytes and modulates cytokine secretion. Exp Hematol 2002;30:1115–1123.

7 Kiyokawa N, Kokai Y, Ishimoto K, Fujita H, Fujimoto J, Hata J: Characterization of the common acute lymphoblastic leukemia antigen (CD10) as an activation molecule on mature human B cells. Clin Exp Immunol 1990;79:322–327.

8 Teixido J, Hemler ME, Greenberger JS, Anklesaria P: Role of beta 1 and beta 2 integrins in the adhesion of human CD34hi stem cells to bone marrow stroma. J Clin Invest 1992;90:358–367.

9 Papayannopoulou T, Priestley GV, Nakamoto B: Anti-VLA4/VCAM-1-induced mobilization requires cooperative signaling through the kit/mkit ligand pathway. Blood 1998;91:2231–2239.

10 Taichman RS, Emerson SG: Human osteoblasts support hematopoiesis through the production of granulocyte colony-simulating factor. J Exp Med 1994;179:1677–1682.

11 Taichman RS, Reilly MJ, Emerson SG: Human osteoblasts support human hematopoietic progenitor cells in in vitro bone marrow cultures. Blood 1996;87:518–524.

12 Ahmed N, Khokher MA, Hassan HT: Cytokine-induced expansion of human CD34+ stem/progenitor and CD34+CD41+ early megakaryocytic marrow cells cultured on normal osteoblasts. Stem Cells 1999;17:92–99.

13 Wodnar-Filipowicz A: Flt3 ligand: role in control of hematopoietic and immune functions of the bone marrow. News Physiol Sci 2003;18:247–251.

14 Drouet M, Mathieu J, Grenier N, Multon E, Sotto J-J, Herodin F: The reduction of in vitro radiation-induced Fas-related apoptosis in CD34+ progenitor cells by SCF, FLT-3 ligand, TPO, and IL-3 in combination resulted in CD34+ cell proliferation and differentiation. Stem Cells 1999;17:273–285.

15 Drouet M, Mourcin F, Grenier N, Leroux V, Denis J, Mayol JF, Thullier P, Lataillade JJ, Herodin F: Single administration of stem cell factor, FLT-3 ligand, megakaryocyte growth and development factor, and interleukin-3 in combination soon after irradiation prevents nonhuman primates from myelosuppression: long-term follow-up of hematopoiesis. Blood 2004;103:878–885.

16 Lataillade JJ, Clay D, Dupuy C, Rigal S, Jasmin C, Bourin P, Le Bousse-Kerdilès MC: Chemokine SDF-1 enhances circulating CD34+ cell proliferation in synergy with cytokines: possible role in progenitor survival. Blood 2000;95:756–768.

17 Murdoch C: CXCR4: chemokine receptor extraordinaire. Immunol Rev 2000;177:175–184.

18 Tokoyoda K, Egawa T, Sugiyama T, Choi B-I, Nagasawa T: Cellular niches controlling B lymphocyte behavior within bone marrow during development. Immunity 2004;20:707–718.

小児腫瘍のグループスタディーと病理

藤本純一郎[*1]　堀江　弘[*2]

はじめに

今から約6年前に各種難治性疾患に関わるエビデンス創出の基盤づくりのための公的研究費投入が開始された．それを受けて，小児がんについても標準的治療法開発を目指した取り組みが開始された．現在，我が国では小児がんの病型ごとの臨床研究グループがつくられ，統一治療プロトコールに基づく臨床試験などが実施されている．各研究グループには数十～200程度の医療施設が参加している．それらの組織体制は種々であるが，運営委員会や幹事会等の運営母体，プロトコール作成や研究立案を行う各種委員会，研究事務局，データセンター，中央診断システム等から構成されている．

上記の組織体制の中で，病理医が関与する場は主として中央診断システムの部分である．その他，臨床研究グループにおける中央診断に関わる業務は様々で，病理診断以外に，遺伝子診断（増幅，欠失，変異，キメラ遺伝子発現等），染色体診断，骨髄スメア等の形態診断，CT・MRI等画像診断，などが存在する．中央診断システムの役割は標準化された診断による試験参加適格性判定や治療層別化判定に関連する情報提供が基本であるが，一部では治療層別化に有用な新規マーカー開発研究や病態解明に結びつく基礎研究も行われる場合がある．病理中央診断については日本病理学会小児腫瘍組織分類委員会の委員の多くが関わってきた．

小児がんは稀少であり，年間の発生数が1,500～2,000程度と予想されることから，これらの症例を効率よく収集するシステムとしても臨床研究グループによる症例のリクルート，その中での中央診断システムは貴重である．また，診断後の余剰検体や研究用検体を保存し，基礎研究の推進に活用する仕組みも確立中である．また，小児がんの年間発生数把握に関する取り組みも始まっている．我が国におけるがん登録に対する取り組みは甚だしく遅れており，小児がん登録についても言わずもがなの状況である．しかしながら上記の臨床研究の推進ならびに予後の著明な改善に伴い，小児がん登録の重要性が増している．

本稿ではこれらの取り組みの現状を紹介する．

Ⅰ．小児がん臨床研究グループの活動

小児がんを扱う我が国の臨床研究グループとして専門家の間で認知されているものは表1に示した7つである．この中で日本小児白血病・リンパ腫研究グループ（JPLSG）が最も規模が大きい．小児血液腫瘍のプロトコールスタディを実施していた既存の4つの臨床研究グループ（CCLSG，JACLS，KYCCSGおよびTCCSG）がインターグループとして結集して形成されたもので，我が国の主たる小児がん治療施設のほとんどが参加している．小児血液腫瘍および血液系関連疾患に対する臨床試験11件を現在実施している（表2）．JPLSGのホームページでの組織図によると，代議員会と運営委員会が運営の中心となっており，その周囲に各種委員会，データセンター，検体センター等が配置されている．血液腫瘍以外の小児固形腫瘍については，基本的には病型ごとに研究グループが形成されている．小児の代表的な固形腫瘍である神経芽腫，横紋筋肉腫，Ewing肉腫，Wilms腫，肝芽腫については，それぞれ，JNBSG，JRSG，JESS，JWiTS，JPLTのグループが形成されている．なお，小児脳腫瘍についてはJPBTCというNPOとして活動している．また，多くの研究グループは何らかの形で公的研究費の支援を受けながら活動している．治療介入型の臨床試験を実施しているグループが大半だが，ガイドライン治療を実施し基盤となる情報収集を目的とした観察研究に近い形の研究もある．

[*1]国立成育医療センター研究所
[*2]千葉県こども病院検査部病理科

0287-3745/08/¥100/頁/JCLS

表1　我が国の主要な小児がん臨床研究グループ

小児がん臨床研究グループ名	対象病型	実施中の試験数	ホームページなどの情報
日本小児白血病・リンパ腫研究グループ（JPLSG）	白血病，悪性リンパ腫など	11	http://jplsg.jp
日本横紋筋肉腫研究グループ（JRSG）	横紋筋肉腫	4	文献1
日本ユーイング肉腫研究グループ（JESS）	Ewing肉腫	1	文献2
日本神経芽腫研究グループ（JNBSG）	神経芽腫	2	http://www.jnbsg.jp/
日本小児肝癌スタディグループ（JPLT）	肝芽腫など	1	http://home.hiroshima-u.ac.jp/jpltstudy/index.html
日本ウィルムス腫瘍スタディグループ（JWiTS）	Wilms腫	1	文献3
日本小児脳腫瘍コンソーシアム（JPBTC）	髄芽腫など	2	http://www.es-bureau.org/contents/consortium/

表2　現在進行中の小児がん関連臨床試験一覧

病型	試験名	研究グループ	試験ID*
急性リンパ性白血病	・乳児急性リンパ性白血病に対する早期同種造血幹細胞移植療法の有効性に関する後期第Ⅱ相試験（MLL03）	JPLSG	
	・小児フィラデルフィア染色体陽性急性リンパ性白血病（Ph＋ALL）に対するimatinib mesylate第Ⅱ相臨床試験（Ph＋ALL04）	JPLSG	C000000290
急性骨髄性白血病	・小児急性前骨髄急性白血病（APL）に対する多施設共同後期第Ⅱ相臨床試験（AML-P05）	JPLSG	UMIN000000645
	・小児急性骨髄性白血病（AML）に対する多施設共同後期第Ⅱ相臨床試験（AML-05）	JPLSG	UMIN000000511
	・ダウン症候群に発症した小児急性骨髄性白血病に対するリスク別多剤併用化学療法の後期第Ⅱ相臨床試験（AML-D05）	JPLSG	UMIN000000989
悪性リンパ腫	・ALCL99（未分化大細胞型リンパ腫を対象としたヨーロッパとの共同研究）	JPLSG	
	・小児成熟B細胞性腫瘍に対する多施設共同後期第Ⅱ相臨床試験（B-NHL03）	JPLSG	C000000317
	・進行期小児成熟B細胞性腫瘍に対する顆粒球コロニー刺激因子（G-CSF）の一次的予防投与の有用性に関する無作為割付比較試験（B-NHL03 G-CSF）	JPLSG	UMIN000000675
	・小児リンパ芽球型リンパ腫stage Ⅰ/Ⅱに対する多施設共同後期第Ⅱ相臨床試験（LLB-NHL03）	JPLSG	
	・小児リンパ芽球型リンパ腫stage Ⅲ/Ⅳに対する多施設共同後期第Ⅱ相臨床試験（ALB-NHL03）	JPLSG	
血球貪食症候群	・Treatment Protocol of the Second International HLH Study（HLH-2004）	JPLSG	
横紋筋肉腫	・横紋筋肉腫低リスクA群患者に対する短期間VAC 1.2療法の有効性および安全性の評価第Ⅱ相臨床試験	JRSG	
	・横紋筋肉腫低リスクB群患者に対する短期間VAC 2.2/VA療法の有効性および安全性の評価第Ⅱ相臨床試験	JRSG	
	・横紋筋肉腫中間リスク群に対するiVAC療法の有効性および安全性に関する多施設共同研究	JRSG	
	・進行性・転移性横紋筋肉腫に対する自家造血幹細胞救援療法を併用した大量化学療法第Ⅱ床試験	JRSG	
Ewing肉腫	・限局性ユーイング肉腫ファミリー腫瘍に対する集学的治療法の第Ⅱ相臨床試験	JESS	
神経芽腫	・進行神経芽腫に対する遅延局所療法早期第Ⅱ相臨床試験	JNBSG	UMIN000000973
	・高リスク神経芽腫に対する標準的治療の後期第Ⅱ相臨床試験	JNBSG	UMIN000001044
肝癌	・小児肝癌に対するJPLT-2治療プロトコール臨床第Ⅱ相試験	JPLT	UMIN000001116
Wilms腫	・本邦における腎腫瘍に対する病期別統一プロトコール治療の完遂率と有効性の評価（JWiTS-2）	JWiTS	
髄芽腫またはテント上PNET	・小児髄芽腫/PNETに対する多剤併用化学療法と減量放射線療法の第Ⅱ相試験	JPBTC	UMIN000000545
	・乳幼児髄芽腫/PNETに対する多剤併用化学療法および大量化学療法の第Ⅱ相試験	JPBTC	UMIN000000546

*：試験IDは以下のサイトで検索した．
UMIN臨床試験登録システム（UMIN CTR）：http://www.umin.ac.jp/ctr/index-j.htm
財団法人日本医薬情報センター（JAPIC）臨床試験データベース：http://www.clinicaltrials.jp/user/cte_main.jsp
国立保健医療科学院 臨床研究〔試験〕情報検索：http://rctportal.niph.go.jp/
国立がんセンターがん情報サービス：http://ganjoho.ncc.go.jp/professional/med_info/clinical_trial/ct0120.html

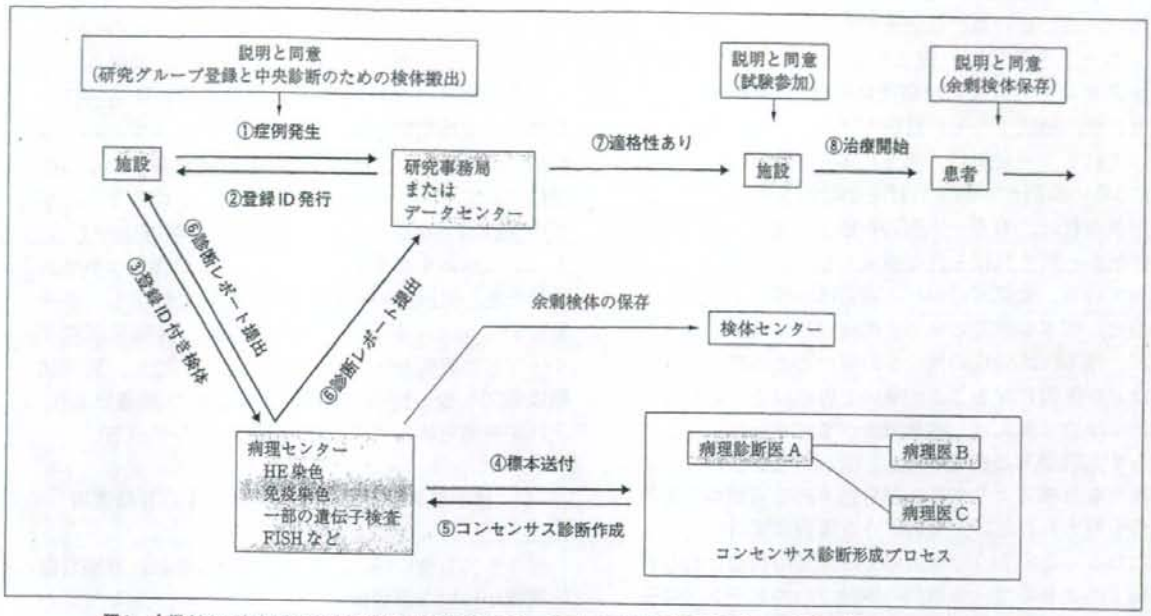

図1　小児がんの臨床試験登録と病理中央診断システム　我が国の小児がん臨床試験で一般的に行われている情報と検体の流れ，その中での病理中央診断システムと余剰検体保存の関連を示す．症例が発症した場合，施設は研究事務局あるいはデータセンターに登録申請を行い登録IDの発行を受ける(①②)．施設は患者検体に登録IDを付けて病理センターに送付する(③)．病理センターは必要な染色等を行った後，指定した病理医に標本を送付する(④)．病理医間でコンセンサス診断を作成し，病理センターを経由して診断レポートを施設ならびにデータセンターに送付する(⑤⑥)．試験参加の適格性の判断が施設に伝えられ治療が開始する(⑦⑧)．なお，このプロセスの中で，患者あるいは代諾者に対して，研究グループ登録と中央診断への検体搬出，試験参加，余剰検体保存，それぞれについて説明が行われ同意が取得される．

小児がんは稀少であるため，スタディクエスチョンを解決するためには，ある程度の症例数が必要となる場合がある．また，新しい臨床試験計画を独自で作成するための国内のエビデンスに乏しい場合もある．そのような場合には，海外で実施されている臨床試験に参加することも視野に入れた研究が展開されている．JPLSGが実施する試験のうち2件(ALCL99およびHLH-2004)は海外との共同研究である．

近年，臨床試験を実施するにあたっては試験内容を登録し公開することを義務づけようとする動きが高まってきている．その理由は，一般にネガティブデータは論文等で公表されない傾向があり，より透明性を確保することを目的としたものである．数年前に欧米の主要雑誌が協調し，事前に試験を登録して公開していない場合は論文掲載を行わない旨の発表を行った．以後，我が国でも登録制度と情報検索のシステムが整備されつつある．上記の研究グループが実施する臨床試験の多くが登録されており概要を検索することができる(**表2**脚注)．

Ⅱ．臨床研究グループと病理中央診断

さて，上記の各臨床研究グループが実施する臨床試験の多くで病理中央診断が実施されている．研究グループごとに複数の専任病理医を定めているが，その多くを日本病理学会小児腫瘍組織分類委員会のメンバーが担当している．病理中央診断の手順は試験ごとに作成される実施計画書に具体的に記載されているが，基本的には以下のごとくである(図1)．まず，試験に該当すると思われる患者が発生した場合，主治医は患者あるいは代諾者に，推測される疾患に該当する臨床試験への参加ならびに中央診断のための検体送付について説明し同意を得る．採取される検体やその処理方法は試験ごとに定められているが，病理中央診断の場合は，HE染色標本は必須で，それ以外に融合遺伝子検索などのため未固定検体の提出を求めているものもある．症例によっては免疫染色用に5～10枚程度の未染薄切標本提出を求めることもある．中央診断の

方法は一般には複数の病理医のコンセンサス診断としてレポートを作成し，標本を提出した施設ならびにデータセンター（または研究事務局）に連絡する．コンセンサス形成プロセスは研究グループごとに若干異なっている．一般には，例えば3名の診断医がいる場合，2名の診断が一致すればその診断を採用する，意見が異なれば，もう一人別の診断医の意見を求め2名の診断が一致すればそれを採用する，といった手法を採っている．意見が分かれる理由は多様である．多くの場合，標本が微量のため全体像がみえない，組織の挫滅，標本作成過程の何らかの理由による質の悪い標本などが原因になることが多いと思われる．純粋に学問的な理由，例えば，疾患概念がまだ十分に固まっておらず主観が入る余地がある．概念が確立されているが新たな指標によりさらに細分化される可能性のある場合も考えられるが，そのような場合は案外少ないと思われる．このような理由による意見の相違はむしろ歓迎すべきもので，多数例の検討でのエビデンス蓄積が重要であるし，研究グループとの連携による中央診断システムはそれらの解明を可能にしうるものである．

Ⅲ．小児腫瘍組織分類委員会の役割

日本病理学会小児腫瘍組織分類委員会は，日本小児外科学会，日本小児科学会からの協同の要請により設置され，1975年の小児腫瘍組織分類図譜第1篇小児肝癌，腎芽腫，神経芽腫群腫瘍の発刊をはじめとして，「癌取扱い規約」に相当する小児がんに関する分類図譜を編集・発行し，我が国における小児がんならびに関連疾患に関わる情報提供を通じて，疾患概念の認識と診断の標準化を目指すことを主たる業務としている．分類図譜はWHO分類や国際的に認知されている学術団体などが公表する最新分類に準拠し，我が国で普及させるための適切な形式に編集して定期的に発行している．以前は，「小児腫瘍組織分類図譜」という名称を使用していたが，2001年発行の版からは「小児腫瘍組織カラーアトラス」と名称変更しかつモダンなデザインの外観としている．

前述のごとく，当委員会のメンバーの多くが小児がんの臨床研究グループの中央診断担当医として参画してきたが，小児腫瘍組織分類委員会としてのまとまった活動ではなく，むしろボランティア的な活動であった．また，臨床研究グループに登録される症例は限られたものであるため，我が国の全体像を把握することはできないといった問題も明らかとなった（ただし，小児悪性リンパ腫の90％程度はJPLSGに登録されていると予想される）．これらの問題を解決する手段として小児腫瘍組織分類委員会が研究グループの中央診断に積極的に関与すると共に，研究に登録されない症例についても，いわばコンサルテーションのような形で中央診断できるシステム構築を現在考慮中である．このシステムを立ち上げるために，小児腫瘍中央診断委員会を小児腫瘍組織分類委員会内部に設置し，症例受付から始まる新診断システム考案，各臨床研究グループとの調整などの活動を開始した．なお，臨床試験に参加しない症例の追跡調査は重要な課題であり，それが実施可能な体制の整備をも目指している．

Ⅳ．診断後の余剰検体や研究用検体の有効活用

言うまでもないが，正確な診断がなされ，詳細な臨床情報が付いた患者検体は研究用リソースとして極めて価値が高い．患者検体を収集する方法を考えた場合，上記のような中央診断システムを利用することが効率的かつ現実的な方法である．実際には中央診断後の残余検体（余剰検体）について患者あるいは代諾者の同意の下に研究用リソースとして保存している場合が多い（図1）．さらには，これら検体は可能な限り一箇所に集約する動きにあり，国立成育医療センター研究所や千葉県がんセンター研究所などが検体センターとして機能している．このような中央診断後の余剰検体のみならず，初めから研究用に採取され使用される検体もある．これらの検体の残余分も貴重なリソースである．現在，臨床試験に関わる余剰検体が順調に集積されてきているが，問題点としては，このような貴重なリソースをどのような取り決めで使用していくかについてのコンセンサスが未だ形成されていない点である．米国最大の小児がん研究グループであるChildren's Oncology Group（COG）では，中央診断システムならびに検体センターをコロンバスにあるNationwide Children's Hospital一箇所に集約し，また，配分ルールもグループ内でのコンセンサスとして決定している．それらも参考にしながら我が国でも共有リソースの使用ルールを決める必要がある．

Ⅴ．米国における小児がん臨床試験と中央診断，検体保存

米国では，数年前に幾つか個別に活動していた小児がん研究グループがCOGという一つの大きな枠組み

の中で活動するようになった．各種レベルの臨床試験の推進のみならず，中央診断システム構築，余剰検体の保存と活用，長期フォローアッププログラムの開発など多角的な活動を展開している．前述のようにCOGにおける中央診断と検体保存のセンターはNationwide Children's Hospital（Columbus Children's Hospitalから最近名称変更，http://www.nationwidechildrens.org）内のBiopathology Center（http://www.biopathologycenter.org）に全て集約されている．そもそもは，同病院病理のStephen J. Qualman博士が始めた事業であるが，現在は極めて高度に発展したシステムとなっている（Qualman博士は昨年引退され，Nilsa C. Ramirez博士が後継者として就任している）．米国には1980年代より全米のがんを対象としたCooperative Human Tissue Network（CHTN，http://www.chtn.nci.nih.gov）がNCIの資金により構築されており，1991年にはすでにPediatric Divisionが出来上がってColumbus Children's Hospitalがセンターとして指名されている．CHTNは検体を収集して中央に保存するというシステムではなく，検体は各施設で保存し情報だけを中央に集めて共有し，必要に応じて配分するというバーチャルバンキングシステムである．現在は，小児がんの多くがCOGの中で診断され治療されるため検体もCOG経由でBiopathology Centerに集められるが，スタディに参加しない症例の検体も有効活用できるシステムとなっている．

COGが行う臨床試験に関わる病理中央診断についても，いったん全ての検体がCOGに集められ，必要な染色等を行ったうえで病型別に定められた病理医に送付されるという形態をとっている．なお，Biopathology CenterにはVIPER（Virtual Imaging for Pathology Education & Research，http://viper.epn.osc.edu/viper/）と呼ぶバーチャルスライドユニットが存在する．オハイオ大学のスーパーコンピュータと共同で開発しており，診断そのもの，診断の標準化および教育といった目的のために活用されている．Biopathology Centerは小児がんのような稀少疾患の研究を推進するための一つの究極の形かもしれない．

Ⅵ．小児がん登録

疾病の基本情報の収集や分析といった地道な活動は我が国では大変立ち遅れている．がん登録もその一つで，昨年成立したがん対策基本法にも盛り込まれず，付帯事項として記載され，がん対策推進計画の中で計画の一つとして表現されるにとどまった．小児がん登録も言わずもがなの状況であり，推進計画の中には言葉としては出てくるが，小児がんを計画に盛り込んでいる自治体は皆無である．地域がん登録は2008年5月現在35道府県市で実施されているがその中で小児がん登録を意識的に位置づけているところは大阪府のみである．ただし，大阪府の場合も意識の高い小児科医の献身的な努力によって支えられているのが現状である．このような状況の中，小児がんの診療に関わる医師たちが学会ベースで小児がんの全数把握に取り組む計画を立案中である．日本小児外科学会（http://www.jsps.gr.jp/public/registration.htm），日本小児血液学会（http://www.jsph.info/osirase/JSPH-touroku.html）ならびに日本小児がん学会（http://www.ccaj-found.or.jp/jspo/general/index.htm）はそれぞれ独自に小児がん登録を実施してきたが，登録率の向上，国際比較の必要性などを考慮し，日本小児がん学会が関連学会と連携して従来より精度の高い小児がん登録を実施する計画を立てている．小児がんの国際比較には，International Classification of Diseases for Oncology 3rd Edition（ICD-O）に基づいたInternational Childhood Cancer Classification 3rd Edition（ICCC-3）[4]が使用されているため，日本小児がん学会が収集する情報を最終的にICCC-3に従って編集できるように現在使用中の登録票ならびに登録方法を改訂中である．

小児がん患者の生存率が70%ないし80%となり長期にわたる生存が期待できる状況となって，小児がん登録に求める役割に変化が起こりつつある．すなわち，二次がん発生やその他の各種晩期合併症の発生をも把握できるシステムづくりを目指すべきとの意見が広まりつつある．国と自治体が連携して推進する地域がん拠点病院構想や学会主導のがん治療認定医制度や認定施設制度の定着と広がりの中で，小児がんについても成人と同じように診療体制の整備が必要であり，小児がん登録もその中に組み込まれるべきものであると考える．

おわりに

我が国における小児がんに関する質の高い臨床研究は始まったばかりと言える．病理医はこのような研究の枠組みの中でかなり重要な役割を演じる必要がある．数年間の経験からは，ある種の小児がん病型では

中央診断と施設診断の間で不一致率が10%を超えるものもあった．これらの情報をいかに現場に還元していくかは中央診断を担当する病理医ならびに小児腫瘍組織分類委員会に課せられた課題であると考える．精度の高い診断を達成するためには，医療現場の病理医の協力が必須であり，今後，学会や書物を通じて小児がんの臨床研究における病理医の活動を広く宣伝，紹介してゆきながら理解を得てゆきたいと考えている．コロンバスのBiopathology Centerの現責任者Ramirez博士との会話では，検体配分についても彼女が大変強い権限をもっていることがわかった．診断のみならず検体保存や配分に際しても病理医は強い指導力を発揮すべきなのだと思う．今後，我が国ではがん診療拠点病院のネットワークが構築されてゆくが，それらの病院では院内がん登録が義務づけられる．そのような場面でも病理医は指導的な役割を発揮するのだと思う．その際，小児がんにもご留意いただけると大変ありがたいと思う次第である．

文　献

1) 森川康英：小児横紋筋肉腫に対する中央病理診断及び遺伝子診断に基づく臨床試験の確立と新規治療法開発に関する研究，がん研究助成金報告書（http://ganjoho.ncc.go.jp/pro/mhlw-cancer-grant/2005/keikaku/17-13.pdf）
2) 国立がんセンターがん対策情報センター：がん情報サービス，小児がんシリーズの冊子「小児のユーイング肉腫について」（http://ganjoho.ncc.go.jp/public/qa_links/brochure/child.html）
3) 越永従道，七野浩之，福澤正洋：小児腎腫瘍における治療成績と方針．小児科診療 2005，68：1643-1650
4) International Classification of Childhood Cancer, 3rd ed., SEER International Classification of Childhood Cancer（http://seer.cancer.gov/iccc/）を参照．また，United Kingdom Association of Cancer Registriesよりダウンロード可能（http://82.110.76.19/coding/iccc3.pdf）

In Vitro Gene Delivery by pDNA/Chitosan Complexes Coated with Anionic PEG Derivatives that Have a Sugar Side Chain

Mayu Hashimoto,[1] Yoshiyuki Koyama,[2] and Toshinori Sato*[1]
[1]*Faculty of Science and Technology, Keio University, 3-14-1 Hiyoshi, Kouhoku-ku, Yokohama 223-8522*
[2]*Department of Home Economics, Otsuma Women's University, Chiyoda-ku, Tokyo 102-8357*

(Received December 10, 2007; CL-071368; E-mail: sato@bio.keio.ac.jp)

The cationic pDNA/chitosan complexes were coated with anionic poly(ethylene glycol) derivatives (PEG-A/C's) that have a sugar side chain. Coating the pDNA/chitosan complex with maltose- or lactose-modified PEG-A/C (Mal–PEG-A/C or Lac–PEG-A/C, respectively) greatly promoted their stability in water and transfection efficiency in vitro.

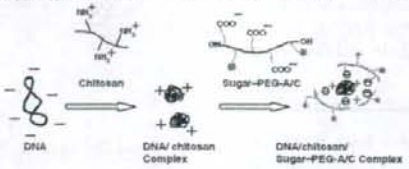

REPRINTED FROM

Chemistry Letters

Vol.37 No.3 2008 p.266–267
CMLTAG
March 5, 2008

The Chemical Society of Japan

Published on the web (Advance View) February 2, 2008; doi:10.1246/cl.2008.266

In Vitro Gene Delivery by pDNA/Chitosan Complexes Coated with Anionic PEG Derivatives that Have a Sugar Side Chain

Mayu Hashimoto,[1] Yoshiyuki Koyama,[2] and Toshinori Sato*[1]
[1]*Faculty of Science and Technology, Keio University, 3-14-1 Hiyoshi, Kouhoku-ku, Yokohama 223-8522*
[2]*Department of Home Economics, Otsuma Women's University, Chiyoda-ku, Tokyo 102-8357*

(Received December 10, 2007; CL-071368; E-mail: sato@bio.keio.ac.jp)

We developed pDNA/chitosan complexes coated with sugar-modified PEG-A/Cs, which are poly(ethylene glycol) derivatives with a side chain of carboxylic acid and sugar. The cationic pDNA/chitosan complexes were coated with anionic sugar-modified PEG-Cs, and anionic ternary complexes were formed. Coating the pDNA/chitosan complexes with maltose- or lactose-modified PEG-A/C (Mal–PEG-A/C or Lac–PEG-A/C, respectively) greatly promoted their stability in water and transfection efficiency in vitro.

A number of cationic polymers have been developed to deliver exogenous genes into cells. Chitosan is a naturally occurring polysaccharide showing low cytotoxicity, biocompatibility, and biodegradability,[1] and is often employed as a gene carrier. Sato et al. reported that DNA/chitosan complexes were uptaken into tumor cells, but not into blood monocytes.[2] Plasmid DNA (pDNA)/chitosan also showed high-level transfection efficiency both in vitro[3] and in vivo.[4] However, the stability of pDNA/chitosan complexes in water was low by self-aggregation and BSA-induced aggregation. To improve the stability and cell-specificity of the pDNA complexes, lactose- and mannose-modified chitosans have been developed as gene carriers.[5]

Poly(ethylene glycol), PEG, has been widely employed for drug delivery systems to prevent non-specific interaction with serum protein and cells. Conjugation of PEG to pDNA/polyethyleneimine (PEI) complexes resulted in a prolonged circulation time after intravenous injection.[6] The conjugation of PEG to pDNA/chitosan complexes increased the stability in water.[7] However, such a conjugation of PEG to the pDNA/chitosan complexes did not enhance their transfection efficiency.

In this study, we employed PEG derivatives with carboxylic acid and sugar moieties (sugar–PEG-A/Cs) as side chains to coat DNA/chitosan complexes. Anionic sugar–PEG-A/Cs form ternary complexes electrostatically with cationic pDNA/chitosan complexes (Figure 1). Sugar–PEG-A/Cs have been employed to coat pDNA/PEI complexes and enhance transfection efficiency.[8] However, it has been reported that PEI induced strong cytotoxicity.[9] The toxicity of a pDNA/PEI complex was about seven times higher than that of a pDNA/chitosan complex.[10] Therefore, in this study, we prepared pDNA/chitosan/sugar–PEG-A/C ternary complexes and evaluated their transfection efficiency in vitro.

Chitosan was obtained from Yaizu Suisankagaku Industry (Shizuoka, Japan). The average molecular weight was 40000, and the degree of deacetylation was 85%. PEG-A/C and sugar–PEG-A/Cs were synthesized according to a previous paper.[8] The substitution degrees of maltose and lactose were 2.9 and 4.4 per molecule, respectively (Figure 1). The molecular weight of Mal–PEG-A/C was 9770, and that of Lac–PEG-A/C was

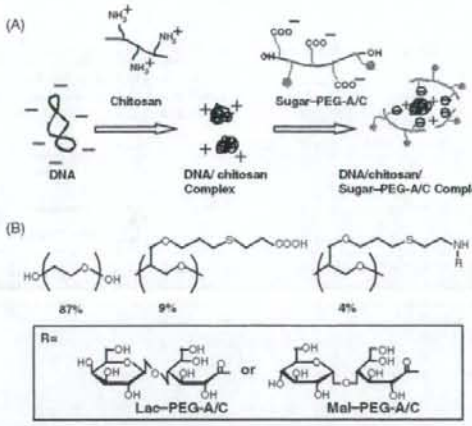

Figure 1. (A) A scheme for the formation of pDNA/chitosan/sugar–PEG-A/C ternary complexes. (B) Structure of sugar–PEG-A/Cs.

10300. A pDNA/chitosan complex was prepared according to the method previously reported.[3] The P/N ratio, which is the ratio of phosphate anion (P) of pDNA to the amino group (N) of chitosan, was 1/5. Ternary complexes were prepared by mixing preformed pDNA/chitosan complexes with aqueous solutions of PEG-A/C or sugar–PEG-A/Cs at appropriate P/N/C (C is carboxyl group of PEG-A/C) ratios for 15 min. In this study, pGL3-Luc (Promega) encoding the *luciferase* gene was employed as pDNA.

AFM observation with SPM-300 (Seiko Instruments Inc., Japan) indicated that the pDNA/chitosan complexes ($P/N > 3$) showed spherical structures of 200 nm in diameter. The morphology and size of the pDNA/chitosan/PEG-A/C complex at $P/N/C = 1/5/20$ were similar to the pDNA/chitosan complex. The particle size of the pDNA/chitosan/sugar–PEG-A/C complex was about 500 nm at $N/P/C = 1/5/10$ and $1/5/20$. There was no obvious morphological difference between the pDNA/chitosan/Mal–PEG-A/C and pDNA/chitosan/Lac–PEG-A/C complexes.

The zeta potential was determined at various P/N/C ratios of the ternary complexes with a ZeeCom (Microtec Co., Ltd., Japan) at 25 °C (Figure 2). The zeta potential of the pDNA/chitosan complex at $P/N = 1/5$ was +49 mV, and was decreased by coating it with sugar–PEG-A/Cs. The zeta potentials of the pDNA/chitosan/sugar–PEG-A/C complexes were negative at $P/N/C = 1/5/10$ and $1/5/20$. Therefore, it is considered that the surface of the cationic pDNA/chitosan complex was coated with anionic Mal–PEG-A/C and Lac–PEG-A/C.

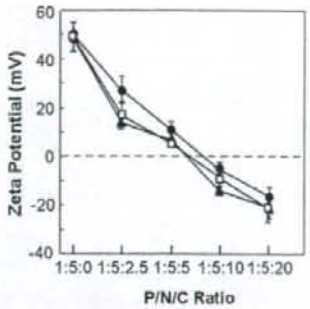

Figure 2. Zeta potentials of pDNA/chitosan/PEG-A/C (closed triangle), pDNA/chitosan/Mal–PEG-A/C (open square), and pDNA/chitosan/Lac–PEG-A/C (closed circle) complexes in 20 mM HEPES buffer. [pDNA] = 1.5 μg/mL.

The resistance of ternary complexes to degradation by DNaseI was investigated by agarose gel electrophoresis. The naked pDNA was completely digested by DNaseI (0.1 U) 50 mM Tris-HCl buffer containing 10 mM $MgCl_2$ and 100 mM NaCl at 37 °C for 30 min. On the other hand, the pDNA/chitosan and pDNA/chitosan/sugar–PEG-A/C complexes showed markedly improved resistance against DNaseI.

Luciferase activities of pDNA/chitosan/PEG-A/C complexes were investigated for B16 mouse melanoma cells. The transfection efficiency of the pDNA/chitosan/PEG-A/C complex at P/N/C = 1/5/2.5 decreased to one tenth that of the pDNA/chitosan complex. The transfection efficiencies of the ternary complexes were recovered by increasing the amount of PEG-A/C, and that of the complex of P/N/C = 1/5/40 was almost comparable with that of the pDNA/chitosan complex.

Next, the transfection efficiencies of the pDNA/chitosan/sugar–PEG-A/C complexes were investigated for B16 cells (Figure 3). The transfection efficiencies of pDNA/chitosan/

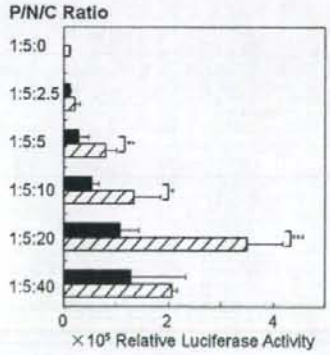

Figure 3. Transfection efficiencies of pDNA/chitosan/Lac–PEG-A/C (black bar) and pDNA/chitosan/Mal–PEG-A/C (cross-hatched bar) complexes at different P/N/C ratios. The luciferase activity of naked pDNA was normalized to 100. The luciferase activity of B16 cells transfected with 2.5 μg of pDNA per 2×10^5 cells represents the mean values of three experiments. The transfection time was 4 h, and post-transfection time was 20 h. * $P < 0.1$, ** $P < 0.05$, *** $P < 0.01$.

Lac–PEG-A/C and pDNA/chitosan/Mal–PEG-A/C complexes at P/N/C = 1/5/20 were 5.5- and 20-fold higher, respectively, than that of the pDNA/chitosan complex. The increased transfection efficiencies of the pDNA/chitosan/sugar–PEG-A/C complexes were also observed for human hepatoma HepG2 cells.

Since both the pDNA/chitosan/Lac–PEG-A/C and pDNA/chitosan/Mal–PEG-A/C complexes showed enhanced transfection efficiencies compared with pDNA/chitosan complexes, it was considered that physicochemical stability contributed to their high transfection efficiency. Thus, the interactions of the DNA complexes with anionic serum albumin and glycosaminoglycan (chondroitin sulfate) were investigated. The turbidity (at 350 nm) of the pDNA/chitosan complex markedly increased depending on the concentration of BSA (0.1–1 mg/mL), whereas those of the pDNA/chitosan/Mal–PEG-A/C complexes were significantly suppressed. Furthermore, the release of pDNA from the pDNA/chitosan and pDNA/chitosan/Mal–PEG-A/C complexes in the presence of 2% chondroitin sulfate was investigated by agarose gel electrophoresis. Though pDNA was released from the pDNA/chitosan complex, no release was observed from the pDNA/chitosan/Mal–PEG-A/C complex. These results suggested that the stability of the pDNA/chitosan complex against polyanions was improved by coating its surface with sugar–PEG-A/Cs. Improvement of the physicochemical stability of chitosan-containing gene carriers would be preferable for in vivo administration.

This work was partly supported by the Special Coordination of Funds for Promoting Science and Technology from the Ministry of Education, Culture, Sports, Science and Technology, Japan (T. S.).

References and Notes

1 S. Hirano, H. Seino, Y. Akiyama, I. Nonaka, *Polym. Eng. Sci.* **1988**, *59*, 897.
2 T. Sato, N. Shirakawa, H. Nishi, Y. Okahata, *Chem. Lett.* **1996**, 725.
3 a) T. Ishii, Y. Okahata, T. Sato, *Biochim. Biophys. Acta* **2001**, *1514*, 51. b) T. Sato, T. Ishii, Y. Okahata, *Biomaterials* **2001**, *22*, 2075.
4 a) K. Roy, H.-Q. Mao, S.-K. Huang, K. W. Leong, *Nature Med.* **1999**, *5*, 387. b) L. Illum, I. Jabbal-Gill, M. Hinchcliffe, A. N. Fisher, S. S. Davis, *Adv. Drug Delivery Rev.* **2001**, *51*, 81.
5 a) M. Hashimoto, M. Morimoto, H. Saimoto, Y. Shigemasa, T. Sato, *Bioconjugate Chem.* **2006**, *17*, 309. b) M. Hashimoto, M. Morimoto, H. Saimoto, Y. Shigemasa, H. Yanagie, M. Eriguchi, T. Sato, *Biotech. Lett.* **2006**, *28*, 815.
6 M. Ogris, S. Brunner, S. Schüller, R. Kircheis, E. Wagner, *Gene Ther.* **1999**, *6*, 595.
7 a) H.-Q. Mao, K. Roy, V. L. Troung-Le, K. A. Janes, K. Y. Lin, Y. Wang, J. T. August, K. W. Leong, *J. Controlled Release* **2001**, *70*, 399. b) I. K. Park, T. H. Kim, Y. H. Park, B. A. Shin, E. S. Choi, E. H. Chowdhury, T. Akaike, C. S. Cho, *J. Controlled Release* **2001**, *76*, 349.
8 Y. Koyama, E. Yamada, T. Ito, Y. Miautani, T. Yamaoka, *Macromol. Biosci.* **2002**, *2*, 251.
9 S. M. Moghimi, P. Symonds, J. C. Murray, A. C. Hunter, G. Debska, A. Szewczyk, *Mol. Ther.* **2005**, *11*, 990.
10 M. Köping-Höggård, I. Tubulekas, H. Guan, K. Edwards, M. Nilsson, K. M. Vårum, P. Artursson, *Gene Ther.* **2001**, *8*, 1108.
11 Supporting Information is available electronically on the CSJ-Journal Web site, http://www.csj.jp/journals/chem-lett.

Published on the web (Advance View) February 2, 2008; doi:10.1246/cl.2008.266

Available online at www.sciencedirect.com
ScienceDirect
Carbohydrate Research 343 (2008) 831–838
Carbohydrate RESEARCH

Glycosylation of dodecyl 2-acetamido-2-deoxy-β-D-glucopyranoside and dodecyl β-D-galactopyranosyl-(1→4)-2-acetamido-2-deoxy-β-D-glucopyranoside as saccharide primers in cells

Toshinori Sato,[a,*] Minako Takashiba,[a] Rumi Hayashi,[a] Xingyu Zhu[a] and Tatsuya Yamagata[b]

[a]*Department of Biosciences and Informatics, Keio University, Yokohama 223-8522, Japan*
[b]*Shenyang Pharmaceutical University, PO Box 29, School of Pharmaceutical Engineering, Shenyang 110016, PR China*

Received 3 July 2007; received in revised form 26 December 2007; accepted 16 January 2008
Available online 26 January 2008

Abstract—Syntheses of oligosaccharides expressed on cells are indispensable for the improvement of the functional analyses of the oligosaccharides and their applications. We are developing saccharide primers for synthesizing oligosaccharides using living cells. In this study, dodecyl 2-acetamido-2-deoxy-β-D-glucopyranoside (GlcNAc-C12) and dodecyl β-D-galactopyranosyl-(1→4)-2-acetamido-2-deoxy-β-D-glucopyranoside (LacNAc-C12) were examined for their abilities to prime the syntheses of neolacto-series oligosaccharides in HL60 cells. When GlcNAc-C12 was incubated with HL60 cells in serum-free medium for 2 days, 14 kinds of glycosylated products were collected from the culture medium. They were separated by high-performance liquid chromatography. The sequences of the products were determined to be neolacto-series oligosaccharides including Lewis^X, sialyl Lewis^X, polylactosamine, and sialylpolylactosamine by mass spectrometry. GlcNAc-C12 was also glycosylated by B16 cells and gave sialyllactosamine. Furthermore, LacNAc-C12 gave similar glycosylated products to GlcNAc-C12.

Keywords: Saccharide primer; *N*-Acetylglucosamine; *N*-Acetyllactosamine; Oligosaccharide; Glycosylation; Animal cells

1. Introduction

The importance of technology to synthesize oligosaccharides expressed on mammalian cells has been indicated by the elucidation of their roles in cell function. We have been developing saccharide primer methods to synthesize oligosaccharides using the glycan biosynthesis system in cells. A saccharide primer is a glycolipid analogue to be glycosylated by cells in culture. Yamagata and co-workers have developed amphiphilic glycolipid analogues such as alkyllactosides.[1,2] Dodecyl β-lactoside (Lac-C12) as a saccharide primer was incorporated into B16 melanoma cells and was glycosylated by glycosyltransferase. The glycosylated product was secreted from the cells. Structural analyses indicated that the product was sialyllactose, which is the carbohydrate portion of GM3 normally expressed on the surface of mouse B16 melanoma cells.

Other primers as substrates for glycosyltransferase in cells have been described in several reports. β-D-Xylosides have been developed as an initiator of glycosaminoglycan biosynthesis.[3,4] Acetylated Xylβ1-6Gal-*O*-2-naphthol and acetylated Galβ1-4GlcNAcβ-*O*-naphthalenemethanol (NM) were investigated as inhibitors of the glycosyltransferase in cells.[5] Furthermore, acetylated Galβ1-4GlcNAcβ-NM and acetylated GlcNAcβ1-3Galβ-NM inhibited the biosynthesis of endogenous sialyl Lewis^X, and they were also glycosylated in human promyelocytic leukemia HL60 cells.[6]

The glycosylation of the saccharide primers was suggested to be dependent on the cell lines, because different types of cells have different intrinsic glycan biosynthesis

* Corresponding author. Tel.: +81 45 566 1771; fax: +81 45 566 1447; e-mail: sato@bio.keio.ac.jp

0008-6215/$ - see front matter © 2008 Elsevier Ltd. All rights reserved.
doi:10.1016/j.carres.2008.01.022

systems. Therefore, a saccharide library could be synthesized by combining various saccharide primers and cells. HL60 cells are known to express ganglioside GM3 and neolacto-series oligosaccharides. When Lac-C12 was incubated with HL60 cells, only the sialylated product (sialyllactose) was obtained, but not neolacto-series oligosaccharides. Therefore, in the present study, we synthesized dodecyl 2-acetamido-2-deoxy-β-D-glucopyranoside (GlcNAc-C12) and dodecyl β-D-galactopyranosyl-(1→4)-2-acetamido-2-deoxy-β-D-glucopyranoside (LacNAc-C12) as saccharide primers (Fig. 1), and the glycosylation reactions of those primers by HL 60 cells and B16 cells were examined.

2. Results

2.1. Glycosylation of GlcNAc-C12 by HL60 cells

HL60 cells were employed to examine the usefulness of GlcNAc-C12 as saccharide primer for the synthesis of neolacto-series oligosaccharides. After incubation of 50 μM of GlcNAc-C12 with HL60 cells, glycosylated products and unreacted primers were collected from the culture medium and cell fraction using a Sep-Pak C_{18} column. The glycosylated products adsorbed to the column were eluted using mixed solvents of methanol and water. The glycosylated products were largely detected from the culture medium. The acidic and neutral products were eluted with 3:7 MeOH–H_2O, and 1:9 MeOH–H_2O, respectively. As shown in Figure 2A, HPTLC (high-performance thin-layer chromatography) indicated that the fractions eluted with 3:7 MeOH–H_2O contained four neutral products (N1–N4), and the fractions eluted with 1:9 MeOH–H_2O contained six acidic products (A1–A6). Next, the neutral and acidic products were separated by high-performance liquid chromatography (HPLC). The four neutral products were separated using 70:28:2 $CHCl_3$–MeOH–H_2O as shown in Figure 2B. N1, N2, N3, and N4 were detected in fraction numbers 7–9, 11–12, 35–40, and 70–80, respectively. The four acidic products (A1–A4) were separated using 70:28:2 $CHCl_3$–MeOH–H_2O as shown in Figure 2C. A1, A2, A3, and A4 were detected in fraction numbers 17–19, 20–23, 26–28, and 45–50, respectively. Two acidic products (A5–A6) were separated using 60:35:5 $CHCl_3$–MeOH–H_2O as shown in Figure 2D. A4 and A5 were detected in fraction numbers 10 and 11–13, respectively.

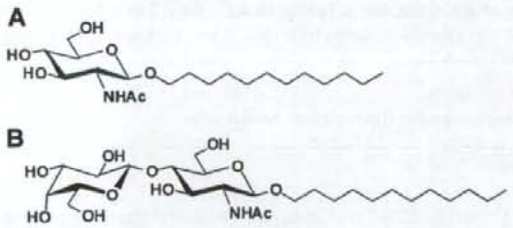

Figure 1. Saccharide primers, GlcNAc-C12 (A) and LacNAc-C12 (B), employed in this study.

2.2. Analyses of the chemical structures of products by mass spectrometry

Analyses of the structures of products separated by HPLC were carried out by MALDI-TOFMS (matrix-assisted laser desorption and ionization time-of-flight mass spectrometry). The observed masses and the deduced sequences of the glycosylated products are shown in Table 1. The mobility of N1 on HPTLC was same as that of synthetic Galβ1-4GlcNAc-C12 (LacNAc-C12), and the non-reducing hexose of N1 was cleaved by jack bean β-galactosidase (data not shown). Furthermore, the positive MALDI-PSD (post-source decay)

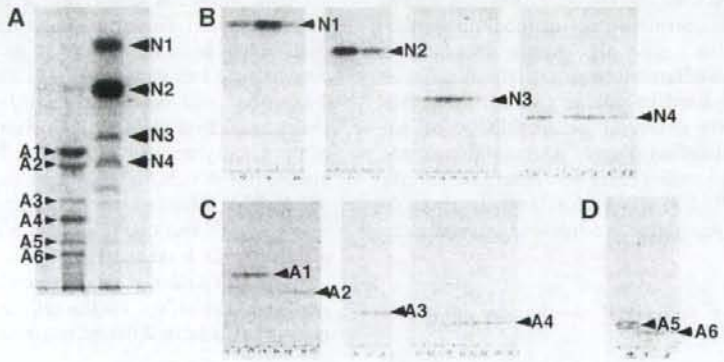

Figure 2. HPTLC of the products collected using a Sep-Pak C_{18} column (A), and purified by HPLC (B, C, and D) for the glycosylation of GlcNAc-C12 by HL60 cells.

Table 1. Deduced sequences and mass observed by MALDI-TOF-MS for the glycosylated products from GlcNAc-C12

Product	Sequence	Observed mass
N1	Galβ1-4GlcNAc-C12	574.1 $[M+Na]^+$
N2	Galβ1-4(Fucα1-3)-GlcNAc-C12	720.1 $[M+Na]^+$
N3	Galβ1-4GlcNAcβ1-3Galβ1-4GlcNAc-C12	939.1 $[M+Na]^+$
N4	Galβ1-4GlcNAcβ1-3Galβ1-4(Fucα1-3)GlcNAc-C12	1085.3 $[M+Na]^+$
A1	NeuNAcα2-3Galβ1-4GlcNAc-C12	841.4 $[M-H]^-$
A2	NeuNAcα2-6Galβ1-4GlcNAc-C12	841.4 $[M-H]^-$
A3	NeuNAc-(Galβ1-4GlcNAc)$_2$-C12	1230.1 $[M-H]^-$
A4	Fucose+A3	1376.3 $[M-H]^-$
A5	NeuNAc-(Galβ1-4GlcNAc)$_3$-C12	1595.9 $[M-H]^-$
A6	Fucose+A5	1742.0 $[M-H]^-$

spectrum (Table 2) revealed a peak at m/z 305.32 corresponding to $^{0,2}A_2$ fragment ($+Na^+$, intramolecular cleavage of GlcNAc). The results of MALDI-PSD agreed with the values in the literature.[7] Thus, N1 was determined to be Galβ1-4GlcNAc-C12. N2 was predicted to be H antigen (Fuc-Gal-GlcNAc-C12) or Lewis^X (Gal-(Fuc)-GlcNAc-C12) from the peak of m/z 720.1 ($[M+Na]^+$) of the MALDI-TOF-MS spectrum (Table 1). The MALDI-PSD spectrum of N2 (Table 2) revealed peaks at m/z 558.4 corresponding to $Y_{1\beta}$ (Fuc-GlcNAc-C12+Na^+) and m/z 305.4 corresponding to the $Y_{1\alpha}/^{0,2}A_2$ fragment ($+Na^+$). The observed fragment ions of N2 were similar to the MALDI-PSD spectrum of Lewis^X reported in the literature.[7] Therefore, N2 was determined to be Lewis^X. N3 was predicted to be Gal-GlcNAc-Gal-GlcNAc-C12 from the peak of m/z 939.1 ($[M+Na]^+$) of the MALDI-TOF-MS spectrum (Table 1). The MALDI-PSD spectrum of N3 (Table 2) revealed peaks at m/z 670.5 corresponding to $^{0,2}A_4$ fragment ($+Na^+$) and m/z 305.3 corresponding to $^{0,2}A_2$ fragment ($+Na^+$), suggesting the existence of two β-(1→4) lactosamine units. N4 was predicted to be fucosylated N3 from the peak of m/z 1085.3 ($[M+Na]^+$) of the MALDI-TOF-MS spectrum (Table 1). The MALDI-PSD spectrum of N4 (Table 2) revealed a peak at m/z 558.6 corresponding to $Y_{1\beta}$ (Fuc-GlcNAc-C12+Na^+), and fragmentation ions were similar to those of N3, suggesting that N4 is Galβ1-4GlcNAcβ1-3Galβ1-4(Fucα1-3)GlcNAc-C12. HL60 cells express FUT4, which transfers fucose to lactosamine.[8] Furthermore, it has been reported that FUT4 preferentially transfers fucose to inner GlcNAc residues.[9] The structure of N5 agreed with that of the endogenous glycan reported in the literature.[8,9]

Though the mobilities of A1 and A2 on HPTLC were different, the MALDI-TOF-MS spectra of them revealed the same mass of 841.4 ($[M-H]^-$), corresponding to NeuNAc-Gal-GlcNAc-C12 (sLacNAc-C12, Table 1). Since A1 and A2 are considered to have different linkages of *N*-acetylneuraminic acid to galactose, the

Table 2. Fragment ions observed by MALDI-PSD spectrum for the glycosylated products from GlcNAc-C12

Product	Fragments
N1	226.4 ($[Y_1/B_2+Na]^+$), 305.3 ($[^{0,2}A_2+Na]^+$), 388.4 ($[B_2+Na]^+$), 412.4 ($[Y_1+Na]^+$),
N2	226.3 ($[Y_{1\alpha}/Y_{1\beta}/B_2+Na]^+$), 305.4 ($[Y_{1\alpha}/^{0,2}A_2+Na]^+$), 370.5 ($[Z_1/B_2+Na]^+$), 388.3 ($[Y_{1\alpha}/B_2+Na]^+$), 412.4 ($[Y_{1\alpha}/Y_{1\beta}+Na]^+$), 534.4 ($[B_2+Na]^+$), 556.4 ($[Z_1+Na]^+$), 558.4 ($[Y_{1\beta}+Na]^+$), 574.6 ($[Y_{1\alpha}+Na]^+$)
N3	226.3 ($[Y_3/B_2+Na]^+$, $[B_4/Y_1+Na]^+$), 305.3 ($[^{0,2}A_2+Na]^+$), 388.2 ($[B_2+Na]^+$ or $[B_4/Y_2+Na]^+$), 406.4 ($[C_2+Na]^+$), 412.5 ($[Y_1+Na]^+$), 550.3 ($[B_3+Na]^+$), 574.5 ($[Y_2+Na]^+$), 670.5 ($[^{0,2}A_4+Na]^+$), 753.7 ($[B_4+Na]^+$), 777.9 ($[Y_3+Na]^+$)
N4	226.4 ($[Y_3/B_2+Na]^+$, $[Y_{1\alpha}/B_4/Y_{1\beta}+Na]^+$), 305.3 ($[^{0,2}A_2+Na]^+$), 388.5 ($[B_2+Na]^+$ or $[Y_{1\alpha}/B_4/Y_2+Na]^+$), 406.5 ($[C_2+Na]^+$), 412.7 ($[Y_{1\alpha}/Y_{1\beta}+Na]^+$), 550.6 ($[B_3+Na]^+$), 558.7 ($[Y_{1\beta}+Na]^+$), 574.9 ($[Y_{1\alpha}/Y_2+Na]^+$), 670.4 ($[Y_{1\alpha}/^{0,2}A_4+Na]^+$), 720.6 ($[Y_2+Na]^+$), 778.0 ($[Y_{1\alpha}/Y_3+Na]^+$), 901.9 ($[Y_3+Na]^+$), 940.0 ($[Y_{1\alpha}+Na]^+$)
A3	388.3 ($[Y_4/B_3+Na]^+$, $[Y_2/B_5+Na]^+$), 406.5 ($[Y_4/C_3+Na]^+$), 412.4 ($[Y_1+Na]^+$), 476.3 ($[B_2+Na]^+$), 550.5 ($[Y_4/B_4+Na]^+$), 574.6 ($[Y_2+Na]^+$), 634.9 ($[^{0,2}A_3+Na+K-H]^+$), 679.6 ($[B_3+Na]^+$), 753.8 ($[B_5/Y_3+Na]^+$), 777.7 ($[Y_3+Na]^+$), 939.8 ($[Y_4+Na]^+$)
A4	336.4 ($[B_1+2Na-H]^+$), 388.4 ($[Y_4/B_3+Na]^+$ or $[Y_{1\alpha}/Y_2/B_5+Na]^+$), 406.5 ($[Y_4/C_3+Na]^+$), 412.3 ($[Y_{1\alpha}/Y_{1\beta}+Na]^+$), 476.5 ($[B_2+Na]^+$), 550.6 ($[Y_4/B_4+Na]^+$), 558.9 ($[Y_{1\beta}+Na]^+$), 574.6 ($[Y_{1\alpha}/Y_2+Na]^+$), 634.9 ($[^{0,2}A_3+Na+K-H]^+$), 679.6 ($[B_3+Na]^+$), 720.9 ($[Y_2+Na]^+$), 777.8 ($[Y_{1\alpha}/Y_3+Na]^+$), 841.3 ($[B_4+Na]^+$), 923.9 ($[Y_3+Na]^+$), 939.6 ($[Y_{1\alpha}/Y_4+Na]^+$), 1085.4 ($[Y_4+Na]^+$), 1230.8 ($Y_{1\alpha}$)
A5	388.1 ($[Y_6/B_3+Na]^+$, $[B_5/Y_4+Na]^+$ or $[B_7/Y_2+Na]^+$), 406.2 ($[Y_6/C_3+Na]^+$ or $[C_5/Y_4+Na]^+$), 550.3 ($[B_6/Y_4+Na]^+$), 574.6 ($[Y_2+Na]^+$), 591.2 ($[Y_5/B_5+Na]^+$ or $[B_7/Y_4+Na]^+$), 596.7 ($[^{0,2}A_3+Na]^+$), 634.9 ($[^{0,2}A_3+Na+K-H]^+$), 670.2 ($[Y_6/^{0,2}A_5+Na]^+$, $[Y_4/^{0,2}A_7+Na]^+$), 679.5 ($[B_3+Na]^+$), 753.6 ($[Y_6/B_5+Na]^+$ or $[B_7/Y_4+Na]^+$), 777.6 ($[Y_3+Na]^+$), 916.8 ($[Y_4+H]^+$), 939.5 ($[Y_4+Na]^+$), 999.8 ($[^{0,2}A_5+Na]^+$), 1045.1 ($[B_5+Na]^+$), 1142.7 ($[Y_5+Na]^+$), 1305.0 ($[Y_6+Na]^+$)
A6	388.6 ($[Y_6/B_3+Na]^+$, $[B_5/Y_4+Na]^+$ or $[Y_{1\alpha}/B_7/Y_2+Na]^+$), 406.8 ($[Y_6/C_3+Na]^+$, $[C_5/Y_4+Na]^+$), 550.5 ($[B_6/Y_4+Na]^+$), 574.9 ($[Y_{1\alpha}/Y_2+Na]^+$), 591.3 ($[Y_5/B_5+Na]^+$ or $[Y_{1\alpha}/B_7/Y_3+Na]^+$), 596.2 ($[^{0,2}A_3+Na]^+$), 634.4 ($[^{0,2}A_3+Na+K+H]^+$), 720.2 ($[Y_2+Na]^+$), 753.8 ($[Y_{1\alpha}/Y_6/^{0,2}A_5+Na]^+$ or $[Y_{1\alpha}/Y_4/^{0,2}A_7+Na]^+$), 777.6 ($[Y_{1\alpha}/Y_3+Na]^+$), 899.9 ($[Y_4/B_7+Na]^+$), 916.9 ($[Y_{1\alpha}/Y_4+H]^+$), 923.9 ($[Y_3+Na]^+$), 939.8 ($[Y_{1\alpha}/Y_3+Na]^+$), 1000.0 ($[Y_{1\alpha}/^{0,2}A_5+Na]^+$), 1045.5 ($[B_5+Na]^+$), 1085.7 ($[Y_4+Na]^+$), 1288.8 ($[Y_5+Na]^+$), 1304.5 ($[Y_{1\alpha}/Y_6+Na]^+$), 1451.0 ($[Y_6+Na]^+$), 1472.6 ($[Y_6+2Na-H]^+$), 1596.1 ($[Y_{1\alpha}+Na]^+$)

enzymatic cleavages of sLacNAc-C12 by neuraminidases were examined. The neuraminidases employed in this study were *Arthrobacter ureafacience* neuraminidase, which hydrolyzes α-(2→3), α-(2→6), and α-(2→8) linkages,[10] and *Macrobdella decora* neuraminidase, which hydrolyzes α-(2→3) linkage.[11] Though *N*-acetylneuraminic acid of A1 was cleaved by both neuraminidases, that of A2 was cleaved by the *A. ureafacience* neuraminidase but not by the *M. decora* neuraminidase. The hydrolyzed products showed the same mobility as synthetic Galβ1-4GlcNAc-C12. Next, ESI (electrospray ionization)-CID (collision-induced dissociation) was employed to distinguish between A1 and A2. The ESI-CID spectra of A1 and A2 showed peaks of *m/z* 887.5 ($[M+2Na-H]^+$) corresponding to NeuNAc-Gal-GlcNAc-C12, and *m/z* 574.3 ($[(M\text{-anNeuNAc})+Na]^+$) corresponding to Y_2 fragment (Gal-GlcNAc-C12). The relative intensity of Y_2 (*m/z* 574.3) to the parent peak (*m/z* 887.5) showed significant differences between A1 and A2, and was 0.68 for A1 and 0.03 for A2. It has been reported that α-(2→3) sialyl linkage was distinguished from α-(2→6) sialyl linkage based on the ESI-CID spectra.[12] In the literature, the fragmentation ions produced by the cleavage of the α-(2→3) sialyl linkage showed much higher intensity than those produced by the cleavage of the α-(2→6) sialyl linkage. Therefore, from the results of enzymatic digestions and ESI-CID spectra, A1 and A2 were determined to be NeuNAcα2-3Galβ1-4GalNAc-C12 and NeuNAcα2-6Galβ1-4GalNAc-C12, respectively.

The MALDI-TOFMS spectra of A3 and A5 (Table 1) revealed peaks of *m/z* 1230.1 ($[M-H]^-$) corresponding to NeuNAc-(Gal-GlcNAc)$_2$-C12 and *m/z* 1571.7 ($[M-H]^-$) corresponding to NeuNAc-(Gal-GlcNAc)$_3$-C12. A3 was considered to be produced by the sialylation of N4. The MALDI-TOF-MS spectra of A4 and A6 revealed peaks of *m/z* 1352.7 ($[M-H]^-$) corresponding to fucosylated A3 and *m/z* 1779.0 ($[M-H]^-$) corresponding to fucosylated A5. The positive-ion mode MALDI-PSD spectrum of A4 (Table 2) revealed peaks at *m/z* 558.9 corresponding to $Y_{1\beta}$ (Fuc-GlcNAc-C12+Na^+) and *m/z* 720.9 corresponding to Y_2 (Fuc+Gal-GlcNAc-C12+Na^+). The positive-ion mode MALDI-PSD spectrum of A6 (Table 2) also revealed a peak at *m/z* 720.2 corresponding to Y_2 (Fuc+Gal-GlcNAc-C12+Na^+), *m/z* 923.9 corresponding to Y_3 (Fuc+GlcNAc-Gal-GlcNAc-C12+Na^+), and *m/z* 1085.7 corresponding to Y_4 (Fuc+Gal-GlcNAc-Gal-GlcNAc-C12+Na^+). These MALDI-PSD spectra suggested that the fucose moieties in A4 and A6 were linked to the innermost GlcNAc residue. It has been reported that HL60 cells express α-(1→3)-fucosyltransferase, and fucosylated monosialyl glycolipids having similar structures to A4 and A6 were detected in HL60 cells.[13] Though the linkages of *N*-acetylneuraminic acid in A3, A4, A5, and A6 could not be determined in the present study, they were inferred to be α-(2→3) from the structural analysis of the sialyl linkage of sialylpolylactosamine expressed in HL60 cells.[14]

2.3. Glycosylation of LacNAc-C12 by HL60 cells

Next, the glycosylation of LacNAc-C12 by HL60 cells was examined. After incubation of HL60 cells with 50 μM LacNAc-C12 for 2 days, glycosylated products and unreacted primer were isolated from the culture medium. The glycosylated products collected using a Sep-Pak C_{18} column were analyzed by HPTLC. One neutral product and six acidic products were detected. The analyses of mobility on HPTLC and the mass spectrum indicated that the products glycosylated from LacNAc-C12 were the same as those from GlcNAc-C12. The neutral product was N2 and the acidic products were A1–A6.

2.4. Comparison of GlcNAc-C12 and LacNAc-C12 as glycosyl acceptors in B16 cells

After incubation of 50 μM GlcNAc-C12 or LacNAc-C12 with B16 cells for 2 days, glycosylated products were isolated from the culture medium. The glycosylated products were analyzed by HPTLC and MALDT-TOF-MS. Using GlcNAc-C12, two glycosylated products were detected. One was Gal-GlcNAc-C12, whose mobility on HPTLC was the same as that of synthetic LacNAc-C12. The other was considered to be NeuNAc-Gal-GlcNAc-C12 (sLacNAc-C12) from the mass spectrum. For LacNAc-C12, the detected product was also suggested to be sLacNAc-C12 from the mobility on HPTLC and from the mass spectrum. To determine the linkage of the sialic acid, the product was treated with neuraminidases from *A. ureafaciens* and *M. decora*. Since the glycosylated product sLacNAc-C12 was hydrolyzed by both sialidases, the linkage of NeuNAc-Gal was determined to be α-(2→3). The amount of sLacNAc-C12 derived from GlcNAc-C12 was two times higher than that from LacNAc-C12, when the dose of saccharide primers was 50 μM (Fig. 3). The glycosylation efficiency of GlcNAc-C12 in cells was higher than that of LacNAc-C12 in cells. When the dose of GlcNAc-C12 was 50 μM (250 nmol), the amount of sLacNAc-C12 was determined to be 7.5 nmol by quantitative analysis using GM1 as standard.

2.5. Cell growth in the presence of saccharide primers

B16 cells were cultured in the absence and the presence of 50 μM GlcNAc-C12 and LacNAc-C12 for 2 days. The cell growth in the presence of the saccharide primers was almost similar to that of control (Fig. 4). Cell growth of HL60 cells was also investigated in the presence of 50 μM GlcNAc-C12 for 2 days (data not

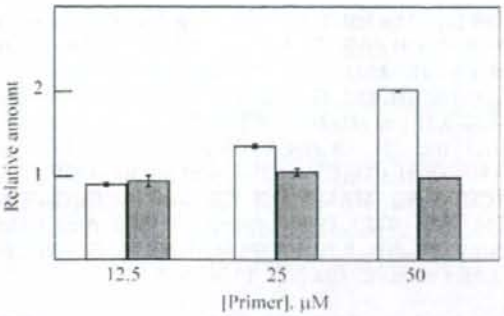

Figure 3. Relative amounts of NeuNAc-Gal-GlcNAc-C12 glycosylated from GlcNAc-C12 (white column) and Gal-GlcNAc-C12 (black column) by B16 melanoma cells (2×10^6 cells). The relative amounts were analyzed by densitometry at 540 nm followed by staining with resorcinol–HCl. The dose of saccharide primers was 50 μM.

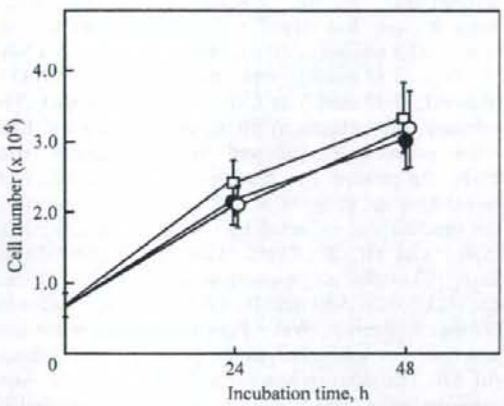

Figure 4. Growth of B16 cells cultured in the absence (closed circle) and the presence of 50 μM GlcNAc-C12 (open circle) and LacNAc-C12 (open square).

shown). The primers showed no cytotoxicity at the present experimental conditions.

3. Discussion

Convenient synthesis of glycan structures present on cells is important for the study to elucidate glycan function. Since saccharide primers can act as substrates for glycosyltransferases present in cells, they are useful for the synthesis of oligosaccharides expressed in cells. Saccharide primers are building blocks for constructing an oligosaccharide library by biocombinatorial synthesis that is combination of different saccharide primers and a variety of cells. It has been reported that Lac-C12, which is a mimicry of lactosylceramide, was useful to synthesize the oligosaccharides of glycosphingolipids (GSL). For example, Lac-C12 gave GM3 oligosaccharide when incubated with B16 melanoma cells. Furthermore, 12-azido dodecyl-β-lactoside (Lac-C12-N3) was synthesized with the aim of preparing glycan arrays or glycopolymers. Lac-C12-N3 was also glycosylated by cells as well as Lac-C12[15] and could be conjugated to solid supports by the modified Staudinger reaction or condensation reaction followed by reduction to the amino group for detecting carbohydrate recognition.[16]

For the construction of oligosaccharide libraries, it is important to synthesize various oligosaccharides. In our ongoing studies, it has been found that Lac-C12 gave rise to various oligosaccharides of ganglio- and globo-series gangliosides. Then, in the present study, we synthesized novel saccharide primers to selectively obtain neolacto-series oligosaccharides. In the biosynthesis of neolacto-series glycans, the lactosamine unit of Galβ1-4GlcNAc is the precursor region for sugar elongation. Thus, saccharide primers containing GlcNAc and LacNAc would be substrates for glycosyltransferases synthesizing neolacto-series oligosaccharides. In the literature, Esko and co-workers have reported that disaccharide primers such as peracetylated Galβ1-4GlcNAc-NM were fucosylated to Galβ1-4(Fucα1-3)GlcNAc-NM, and peracetylated GlcNAcβ1-3Gal-NM was converted to Galβ1-4(Fucα1-3)GlcNAcβ1-3Gal-NM, NeuNAcα2-3Galβ1-4GlcNAcβ1-3Gal-NM, and NeuNAcα2-3Galβ1-4(Fucα1-3)GlcNAcβ1-3Gal-NM by U937 human histiocytic lymphoma cells.[6] Those peracetylated primers were glycosylated after deacetylation in cells. In our study, deacetylated saccharide primer was used for the synthesis of oligosaccharides by cells. GlcNAc-C12 and LacNAc-C12 gave Le^X, sLe^X, polylactosamine, sialylated polylactosamine, and sialylated/fucosylated polylactosamine by incubating with HL60 cells. These oligosaccharides were similar to endogenous glycans observed in HL60.[17] The complex glycosylated products were clearly separated by HPLC, and their chemical structures were determined by enzymatic digestion and mass spectrometry. Separation and structural elucidation of the products were very convenient compared to the endogenous GSLs because the saccharide primers had a uniform aglycon structure.

Since GlcNAc-C12 gave similar glycosylated products to LacNAc-C12, we could conclude that monosaccharide primers as well as disaccharide primers are useful for the synthesis of oligosaccharides. It has been reported that the glycosylation efficiencies of saccharide primers were dependent on their hydrophilic–hydrophobic balance.[2,18] More hydrophilic saccharide primers cannot be internalized into cells, while more hydrophobic ones are strongly adsorbed to the cell membrane. Although the glycosylation efficiency of GlcNAc-C12 was higher than that of LacNAc-C12 in the present study, the structure for giving optimum glycosylation